Optica Applicata, Vol. XXXVIII, No. 3, 2008

Fiber Bragg grating and long period grating sensor for simultaneous measurement and discrimination of strain and temperature effects

KAMINENI SRIMANNARAYANA[1*], MADHUVARASU SAI SHANKAR[1*], RAVINUTHALA L.N. SAI PRASAD[2*], T.K. KRISHNA MOHAN[2], S. RAMAKRISHNA[2], G. SRIKANTH[2], SRIRAMOJU RAVI PRASAD RAO[3*]

[1]Photonics Labs, Department of Physics, National Institute of Technology, Warangal-506 004, India

[2]Department of Physics, National Institute of Technology, Warangal-506 004, India

[3]Department of Physics, Kamala Institute of Technology and Science, Huzurabad, Karimnagar-505 486, India

[*]Corresponding authors: K. Srimannarayana – ksn@nitw.ernet.in, M. Sai Shankar – mb2shankar@yahoo.co.in, R.L.N. Sai Prasad – saiprasad_rlns@yahoo.co.in, S. Ravi Prasad Rao – ravi_kits@rediff.com

Fiber Bragg grating sensors are novel in the determination of various physical parameters. In the case of fiber Bragg grating, on a single measurement of wavelength shift, it is impossible to differentiate between the effects of changes in strain and temperature. The simulation of fiber Bragg grating, long period grating characteristics and use of the different strain-temperature response of combined sensor for the simultaneous measurement and discrimination of strain and temperature in *C* band are demonstrated.

Keywords: fiber Bragg grating, long period grating, discrimination of strain and temperature.

1. Introduction

Fiber Bragg grating (FBG) consists of periodically spaced modulated refractive index zones in an optical fiber. The Bragg wavelength of a grating λ_B, is a function of the effective index of guided mode n_{eff} and period of index modulation Λ given by $\lambda_B = 2n_{\text{eff}}\Lambda$ [1]. The reflected wavelength is also a function of the parameters like temperature, strain, pressure, *etc*., which upon proper calibration, enables accurate measurement of these parameters. However, the technical drawback of this FBG sensor is its inability to distinguish between the shifts in wavelength caused by the strain or temperature.

The second class of Bragg gratings are long period gratings (LPGs), which have the period in the range of hundreds of micrometers. The transmitted peak wavelength

is given by $\lambda_i = (n_{01} - n_{\text{clad}}^{(i)})\Lambda$, where n_{01} is the effective index of the core mode and $n_{\text{clad}}^{(i)}$ is the effective index of the i-th axially symmetric cladding mode [2]. LPG has the larger temperature and smaller strain response compared to those of FBG. In principle, a sensor with an LPG and single FBG can be realized for the measurement of strain and temperature, but firstly, the LPG has larger bandwidth leading to uncertainty in the determination of its central wavelength. The second drawback lies in the complex setup for determining the transmission spectrum of LPG, compared to the interrogation of FBGs narrow reflection spectrum. Hence, in this study, a complex sensor consisting of an LPG followed by two FBGs for simultaneous measurement and discrimination of strain and temperature effects has been employed.

2. Simulation of FBG and LPG and their characteristics

Theoretically, the normalized reflection produced by an FBG is given by [3]

$$R = \frac{\sinh^2\left[\kappa L\sqrt{1-\left(\frac{\delta}{\kappa}\right)^2}\right]}{\cosh^2\left[\kappa L\sqrt{1-\left(\frac{\delta}{\kappa}\right)^2}\right]-\left(\frac{\delta}{\kappa}\right)^2} \tag{1}$$

where L is the grating length, κ is the coupling coefficient, δ is the detuning parameter and δ/κ is the detuning ratio. The detuning parameter for Bragg grating of period Λ is $\delta = \Omega - (\pi/\Lambda)$ where $\Omega = 2\pi n_{\text{eff}}/\lambda$. For sinusoidal variation in the index perturbation, the coupling coefficient for the 1-st order for unblazed Bragg grating is $\kappa = \pi\eta/\lambda_B$ [4], where η is the overlap integral between the forward and reverse propagating guided modes calculated over the fiber core of Bragg grating. In this case, $\eta = \Delta n F$, F is the fractional modal power in the core given by $F = [1 - (1/V^2)]$ where V is the normalized frequency and Δn is the amplitude of induced refractive index perturbation. The normalized power transmitted by the fundamental guided mode through the LPG is given by [5]

$$T = \frac{\cos^2\left[\kappa^{(m)}L\sqrt{1+\left(\frac{\delta^{(m)}}{\kappa^{(m)}}\right)^2}\right]+\left(\frac{\delta^{(m)}}{\kappa^{(m)}}\right)^2}{1+\left(\frac{\delta^{(m)}}{\kappa^{(m)}}\right)^2} \tag{2}$$

where m is the mode number and all the specified parameters in the above case now depend on m.

Using Equation (1), the reflection spectrum of FBG is simulated and drawn using MATLAB. The variations in these spectra were demonstrated by varying the parameters

like grating length and index difference for an FBG with $\Delta = 0.0036$, $n_{core} = 1.45$, core radius of 4.5 μm and grating period of 0.534 nm. It is observed that the spectral bandwidth of the gratings decreased with an increase in the grating length. For a 10 mm long uniform grating, the bandwidth is approximately 0.16 nm and for 20 mm long grating, the bandwidth is reduced to 0.084 nm, as shown in Fig. 1. Further, if the refractive index change is varied, keeping the length of the grating constant, it is observed that, by changing the index of refraction to half the value of the first grating, the reflectivity decreased to approximately 60% and the bandwidth decreased considerably, as shown in Fig. 2. It is observed that the bandwidth approaches a minimum value and remains constant for further decrease in the index of refraction change Δn. The transmission spectrum of the LPG is simulated using Eq. (2) and is shown in Fig. 3.

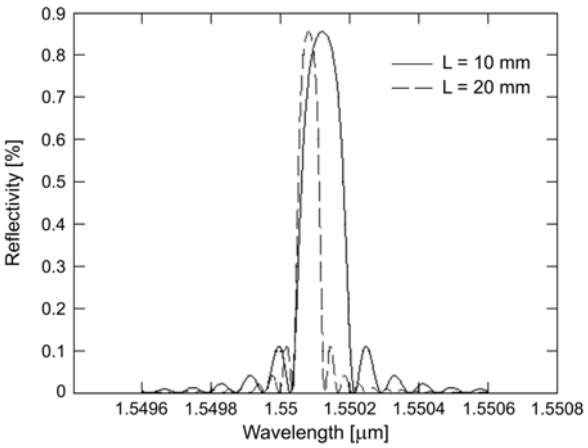

Fig. 1. Spectral profiles for uniform fiber Bragg gratings with different grating lengths.

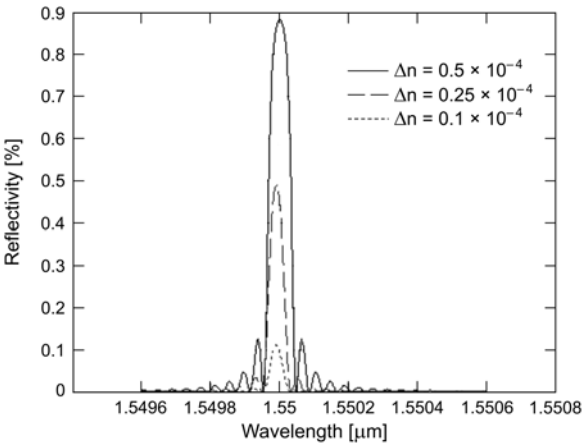

Fig. 2. Spectral profiles for uniform fiber Bragg gratings with different refractive index change.

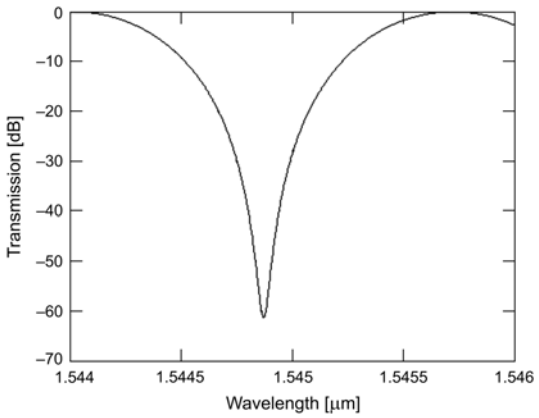

Fig. 3. Transmission spectrum of the LPG.

In the case of the FBGs, the wavelength shift induced by the applied strain ε at a constant temperature is given by [1]

$$\Delta\lambda_B = \lambda_B(1 - P_e)\varepsilon \tag{3}$$

where P_e is the photoelastic coefficient of the fiber. For a temperature change ΔT, the corresponding wavelength shift is given by [1]

$$\Delta\lambda_B = \lambda_B\left[\frac{1}{\Lambda}\frac{\partial\Lambda}{\partial T} + \frac{1}{n}\frac{\partial n}{\partial T}\right]\Delta T = \lambda_B(\alpha + \xi)\Delta T \tag{4}$$

where α is the thermal expansion coefficient and ξ is the thermooptic coefficient.

The response of LPG depends on the change in the grating period and on the differential change in core and cladding indices of the refraction and it also depends on fiber type [2].

When a sensor having one LPG and two FBGs is strained or is under temperature fluctuations, a change in reflected power peaks of FBGs R_1 and R_2 occurs. A change in strain leads to a small decrease in R_1 and small increase in R_2, because the shift in λ_{LP} (peak transmission wavelength of LPG) lags the shift in λ_{B1} and λ_{B2}. However, a change in temperature produces a large increase in R_1 and large decrease in R_2, because the shift in λ_{LP} leads the shifts in λ_{B1} and λ_{B2}. Figures 4 and 5 show typical changes in the reflected powers of FBG peaks due to strain and temperature variations. To analyze the reflectance signals, the function $F(R_1, R_2)$ is calculated using the relation

$$F(R_1, R_2) = \frac{\sqrt{R_1} - \sqrt{R_2}}{\sqrt{R_1} + \sqrt{R_2}} \tag{5}$$

Since the LPG transmission *vs*. wavelength is approximately linear over the region that the FBG and LPG overlap, the difference of $\sqrt{R_1}$ and $\sqrt{R_2}$ is linearly proportional to the amount by which λ_{LP} leads or lags λ_{B1} and λ_{B2}. The square root is required

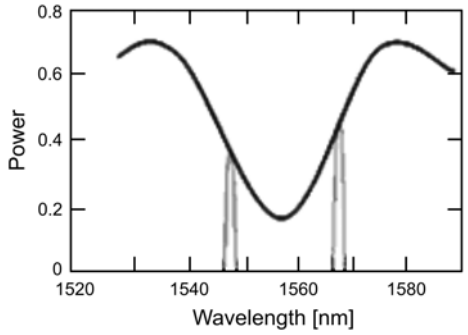

Fig. 4. Change in the reflected powers of FBG peaks with strain.

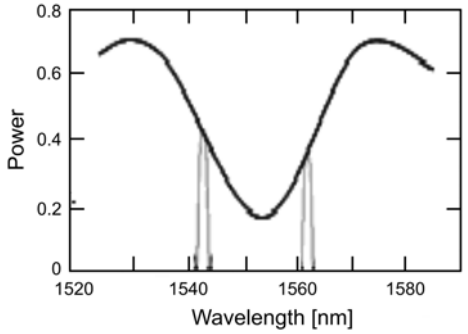

Fig. 5. Change in the reflected powers of FBG peaks with temperature.

because the light passes two times through the LPG. The denominator is normalization constant. This minimizes the fluctuations caused in the total optical power reaching the interrogator. For ease of calculation, a system of two equations

$$\Delta F = A\Delta\varepsilon + B\Delta T$$

$$\Delta\lambda = C\Delta\varepsilon + D\Delta T$$

relating the change in F and the change in one of the FBG wavelengths due to strain and temperature changes (A, C and B, D are the strain and temperature coefficients, respectively) $\Delta\varepsilon$ and ΔT can be solved by

$$\begin{bmatrix} \Delta F \\ \Delta\lambda \end{bmatrix} = \begin{bmatrix} A & B \\ C & D \end{bmatrix} \begin{bmatrix} \Delta\varepsilon \\ \Delta T \end{bmatrix}$$

3. Experimental details

A hybrid FBG/LPG sensor formed on SMF-28 supplied by O/E Land, Canada, with the specifications LPG: L = 15 mm, λ_{LP} ~ 1554 nm; FBG1: L = 12 mm, λ_{B1} ~ 1548 nm; and FBG2: L = 12 mm, λ_{B2} ~ 1560 nm, has been used in this experimental study. The light from the broadband source coupled into the SM fiber with the above sensors, passes through the LPG and gets reflected back from the two FBGs (see Fig. 6).

Fig. 6. Experimental setup for simultaneous application of strain and temperature.

The wavelengths of the two FBGs were chosen at nearly 50% of the transmission peak of the LPG on either side, so that the variation of relative intensities of the FBGs will be linear to the change of the LPG. Upon reflection, the light retraces the LPG and the reflected spectrum is observed on the Interrogator Sensing system (OEFSS-100 supplied by O/E Land, Canada). The two normalized reflected peaks R_1 and R_2 were found by averaging the heights with stored trace of the source spectrum, so that any false variations in R_1 and R_2 are checked due to the change in source spectrum *vs*. wavelength.

In the experimental setup, a microcontroller operated temperature chamber which can be maintained at the desired temperature for the specific time requirement is employed and one end of the fiber is mounted on a motorized actuator (Newport) with computer interface, for applying the strain. The sensor is calibrated by applying known temperatures and strains, and the shift in one of the FBG wavelength and change in $F(R_1, R_2)$ are determined. In order to minimize the effect of thermal expansion of the fiber, the latter was heated locally, while the strain was applied over the longer

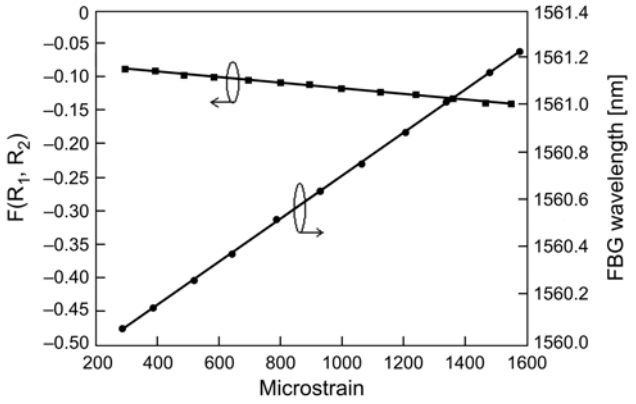

Fig. 7. Variation of $F(R_1, R_2)$ and FBG2 wavelength with strain.

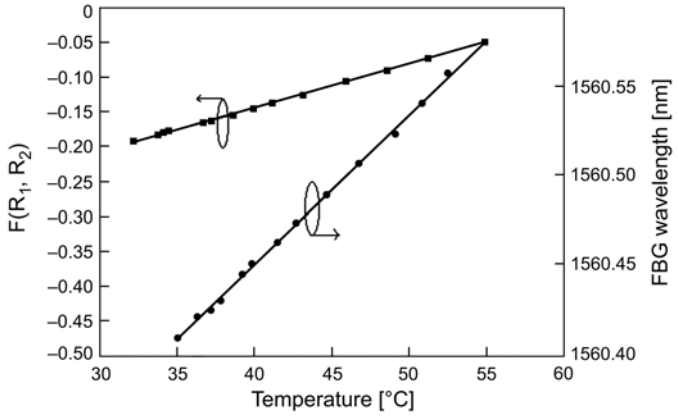

Fig. 8. Variation of $F(R_1, R_2)$ and FBG2 wavelength with temperature.

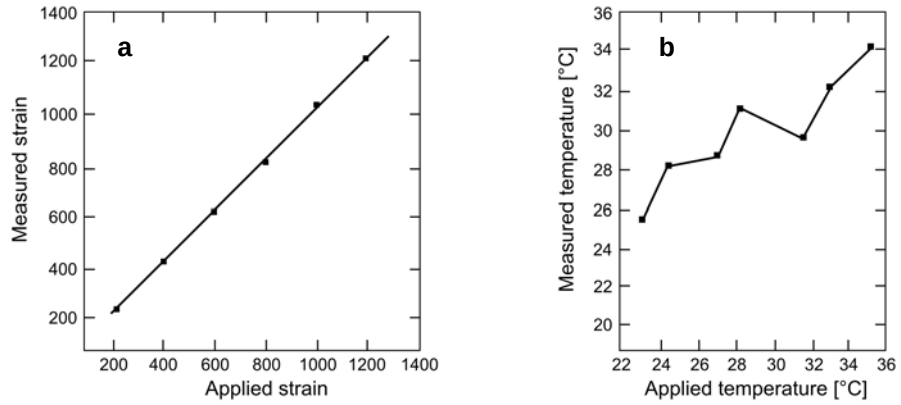

Fig. 9. The rms deviation of the applied and measured strain (**a**), the rms deviation of the applied and measured temperature (**b**).

section of it. The experimental results were plotted in Figs. 7 and 8 for one of the Bragg wavelengths λ_{B2} depicting the variation of the function $F(R_1, R_2)$ and the shift of the Bragg peak λ_{B2} with the strain and temperature, respectively. From the average values of the slopes and also the values of $F(R_1, R_2)$ and λ_{B2} at zero strain and 0 °C, a set of two linearly independent equations were developed which can be conveniently written in the form:

$$\begin{bmatrix} F(R_1, R_2) - 0.35108 \\ \lambda_{B2} - 1559.97 \end{bmatrix} = \begin{bmatrix} -4.8 \times 10^{-5} & 6.52 \times 10^{-3} \\ 0.0946 \times 10^{-3} & 8 \times 10^{-3} \end{bmatrix} \begin{bmatrix} \Delta\varepsilon \\ \Delta T \end{bmatrix}$$

In the experiment, the applied strain was increased from 100–1600 microstrain while the applied temperature was varied between 20–60 °C. To show the quality of

the sensor over this wide range of temperature and strain, measured strain versus applied strain was plotted along with simultaneously measured temperature versus applied temperature in Figs. 9**a** and 9**b**, respectively. The deviation of the measured strain from the applied one was found to be ±11 microstrain. Similarly, the measured and the applied temperatures were compared and the deviation was found to be ±2 °C.

4. Conclusions

A better approach for the accurate measurement of strain and temperature simultaneously with high accuracy has been simulated and demonstrated. The hybrid sensor has the advantage of using the properties of both the FBG and LPG sensors, which in turn, improves its calibration. However, the sensor performance depends on the precision of the grating parameters and the accuracy of the applied strain and temperature for better calibration and the use of sophisticated interrogator system.

Acknowledgement – This work was funded by the Department of Information Technology (DIT) of the Ministry of Communication and Information Technology, the Government of India, New Delhi, India.

References

[1] HILL K.O., MELTZ G., *Fiber Bragg grating technology fundamentals and overview*, Journal of Lightwave Technology **15**(8), 1997, pp. 1263–76.
[2] VENGSARKAR A.M, LEMAIRE P.J., JUDKINS J.B., BHATIA V., SIPE J.E., ERDOGAN T., *Long-period fiber gratings as band-rejection filters*, Journal of Lightwave Technology **14**(1), 1996, pp. 58–65.
[3] SYMS R., COZENS J., *Optical Guided Waves and Devices*, McGraw-Hill, England 1992.
[4] KASHYAP R., *Photosensitive optical fibers: devices and applications*, Optical Fiber Technology **1**(1), 1994, pp. 17–34.
[5] HALL D.G., *Theory of waveguides and devices*, [In] *Integrated Optical Circuits and Components*, [Ed.] L.D.Huctheson, Marcel-Dekker, New York 1987.

Received June 22, 2007